CHAPTER – 5

FIELD EVIDENCE OF LATE QUATERNARY SURFACE FAULTING

The KHF located in the Kachchh Mainland, is an E-W trending, high angle reverse fault characterized by a south-dipping fault plane along which the southern block comprising of solid older Mesozoic rocks (Jumara and Jhuran Formations) had moved upwards with respect to the northern block comprising of relatively softer rocks of Bhuj Formation, as a consequence of the reactivation of the fault during the post-rift inversion phase of the geological evolution of the Kachchh basin (Biswas, 1987). The north facing scarps present on the southern side of KHF display very less amount of aeolian miliolite sedimentation due to its steepness. In addition to this, much of the miliolite sedimentation is either eroded owing to its high erodibility (Talati and Bhatt, 2018b) and anthropogenic modifications of the landscape around the KHF zone. These changes in the KHF zone have given rise to patchy and scattered occurrences of miliolite deposits, which in turn has exposed the underlying Mesozoic rocks. The expression of faulting recorded in the Mesozoic outcrops along KHF is displayed at some locations such as SE of Mankuva (west), south of Shiv paras, and along Ashapura volclay road near Ler village (east). It can be observed that the KHF shows approximately east-west trending strike with slightly variable dip amounts of 52°, 69° and 83° due S respectively at these locations (Figure 5.1). Near SE of Mankuva in Figure 5.1a, the TV tower observed at a distance (shown by arrow) in the photograph is constructed in the KHF zone. The foot-hill region of the KHF scarp can be seen on the southern side of the TV tower, which is mostly covered by alluvium and masks the expression of the fault plane in the Mesozoic rocks. The Mesozoic fault plane exposed near south of Shiv Paras area (Figure 5.1b) shows the KHF plane with roughly E-W trending strike and dipping ~69° due S, along with the exposure of the foot-hill region of the KHF scarp towards the southern direction. Another exposure of the contact between the sandstone of Jhuran Formation and Bhuj Formation (Figure 5.1c) denotes the presence of the KHF plane located on the Ashapura volclay road near Ler village. The scarp can be noticed in the background, which is devoid of miliolite deposits in its foot-hill region. Patidar et al. (2008) also reported several distinct field photographs of the fault plane of KHF exposed in the Mesozoic rocks with variation in dip amount along the strike of the fault plane from west to east at different locations like, SE of Samatra, south of Bharasar, north of Tapkeshwari and towards north of Khatrod peak. At these locations, it can be observed that the dip amount of

KHF plane is comparatively lower (~45°) at the places located towards the western side (SE of Samatra), and it gradually increases (~80°) and tends to get steeper towards the eastern side (north of Khatrod peak) (Patidar et al., 2008).

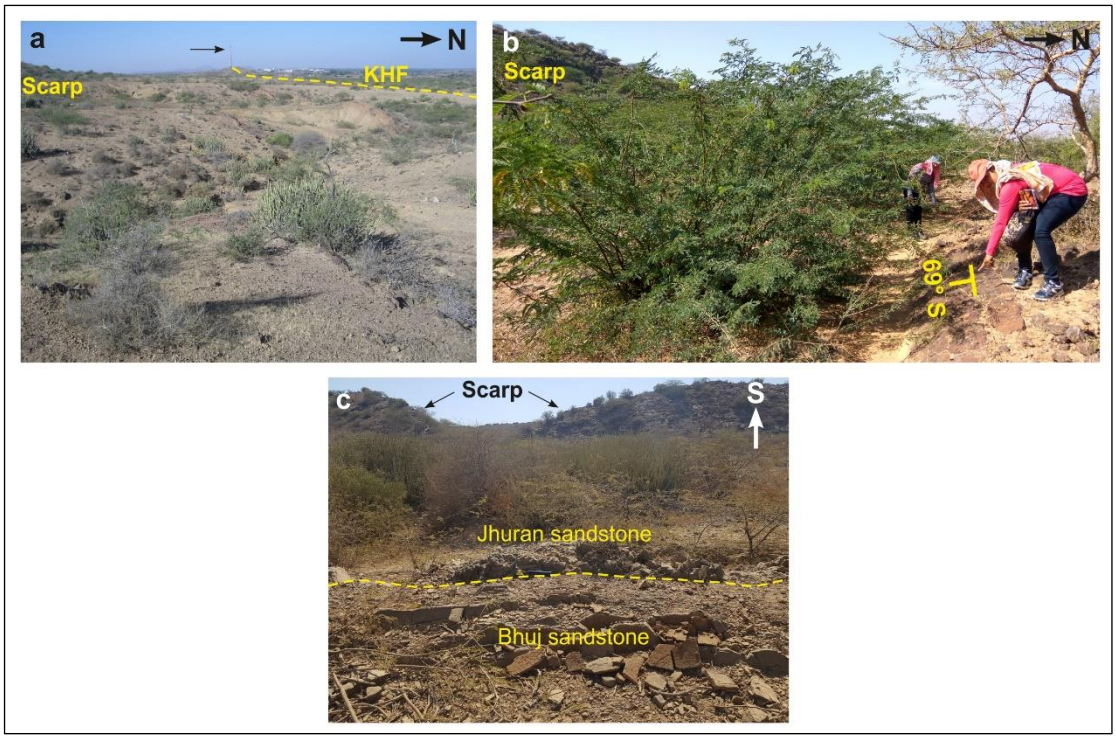

Figure 5.1 Katrol Hill Fault (KHF) plane exposed in the Mesozoic rocks **a.** View of the fault trace of the KHF with scarp in the background found SE of Mankuva. Small arrow points to TV tower. **b.** Field photograph of the exposure of KHF. Note the south dipping fault plane and lithotectonic contact between the sandstone of Bhuj Formation and shale belonging to Jhuran Formation found south of Shiv Paras area. **c.** Field photograph of the KHF plane which marks the contact between the sandstone of Jhuran Formation and Bhuj Formation located near Ler village.

The fault plane, which is exposed in the hard rocks can be identified, studied and mapped without facing much difficulty, for e.g., the south dipping KHF plane, which is exposed in Mesozoic rocks at some locations towards the north of the scarps (Figure 5.1). The study and mapping of historical surface ruptures, especially those that occurred in the instrumental era is relatively simpler. In contrast, surface rupture that occurred in the pre-historical times before the commencement of instrumental era requires diverse geological methods for its recognition and mapping. This is also true for faults that have long recurrence intervals or faults that do not have a known seismic history, for e.g., the Lavic Lake fault (Treiman et al., 2002). Erosional processes, poorly preserved scarps, burial under young

sediments, occurrence of fault strands due to post-depositional processes etc. can make the recognition and mapping of the surface rupture complex (Quigley et al., 2012).

Detailed field work with the main focus on the outcrops of Late Quaternary sediments (Figure 5.2) was carried out for examining the presence of surface faulting or deformation related to faulting and establishing the continuity of the rupture spatially along the KHF in order to constrain the length of Late Quaternary surface faulting.

No other comparable section showing clear offset in Quaternary layers, as observed in the Khari river section (Figure 5.3) was found along the entire length of the KHF primarily due to removal of the thin sedimentary cover by erosional and anthropogenic processes. However, isolated and patchy exposures of deformation in Quaternary sediments are observed at the locations described in the following paragraphs.

The KHF zone shows a largely rocky landscape with south dipping fault plane exposed in Mesozoic rocks almost all along its length in the front of the scarps (Patidar et al., 2007). Patchy outcrops of Quaternary sediments in the KHF zone show very limited stratigraphic units while most consist of aeolian miliolite only (Patidar et al., 2007; Maurya et al., 2017a). All outcrops of Quaternary sediments overlying the KHF were examined as it was necessary to identify and constrain the surface characteristics of the KHF. The present study confirms that the Khari river section, first reported by Patidar et al. (2008) and located exactly over the fault trace of KHF, is stratigraphically the most complete and well-preserved section exposed on the left bank of the north-flowing Khari river, located ~7 km SSW of Bhuj city (Figure 5.3a). The section shows maximum number of Quaternary stratigraphic units exposed at a single location and is also faulted (Figure 5.3). In the following section, the Khari river section, which shows unambiguous evidence of Late Quaternary surface faulting is described in detail.

KHARI RIVER SECTION

At this location, the Quaternary sediment of the Khari river terrace is offset in a dip-slip manner by ~8 m along a gently southward dipping fault plane. The lithotectonic contact between the Bhuj and pre-Bhuj formation of Mesozoic age are exposed at the riverbed and marked as an older fault plane of the KHF (Figure 5.3a). The steeply dipping reverse fault is seen in the Mesozoic rocks at the riverbed, which splays into two planes (F1 & F2) during its upward propagation in the overlying unconsolidated Quaternary sediments. The dip of the fault plane is relatively gentler upwards in the Quaternary section.

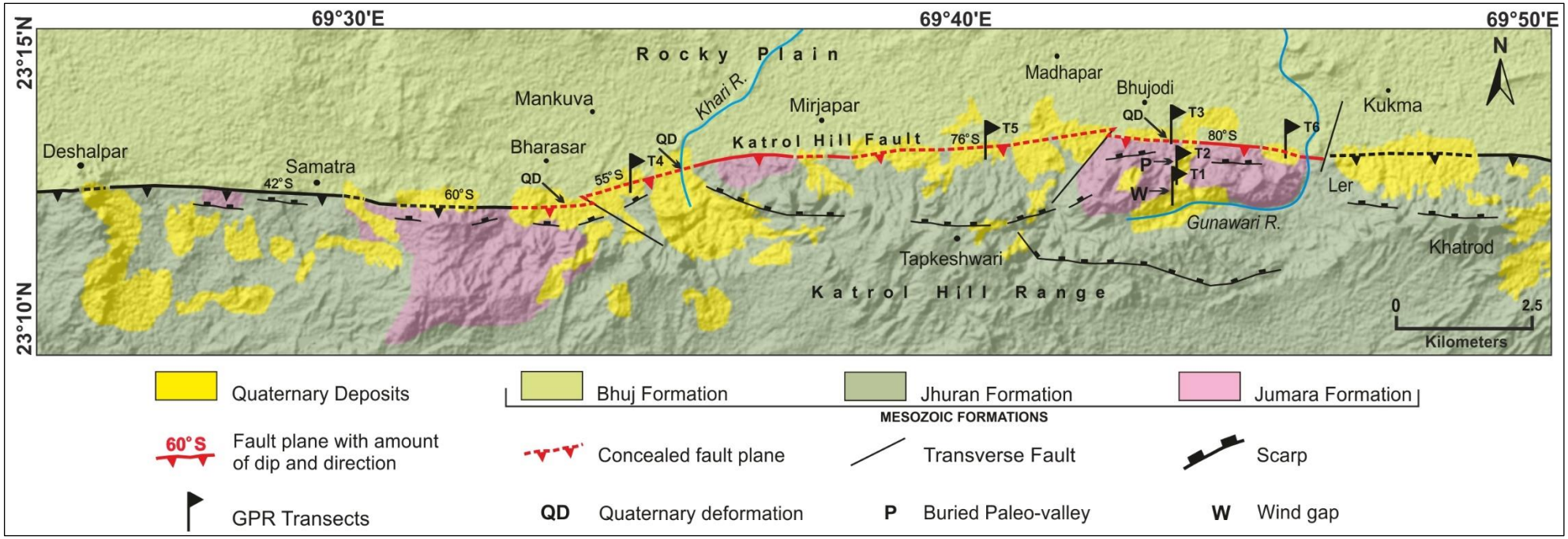

Figure 5.2 Geological map of the study area overlapped on DEM showing the KHF, mapped Quaternary sediments, various geomorphic indicators of neotectonic reactivation of KHF, location of GPR transects (T1 to T6). Red coloured fault line shows active trace of the KHF based on present study. Note the discontinuous nature of Quaternary sediment cover.

The exposed Khari river cliff section and its interpreted section is shown in Figure 5.3b, along with various stratigraphic units, KHF fault plane and associated deformation features shown in Figure 5.3c to g.

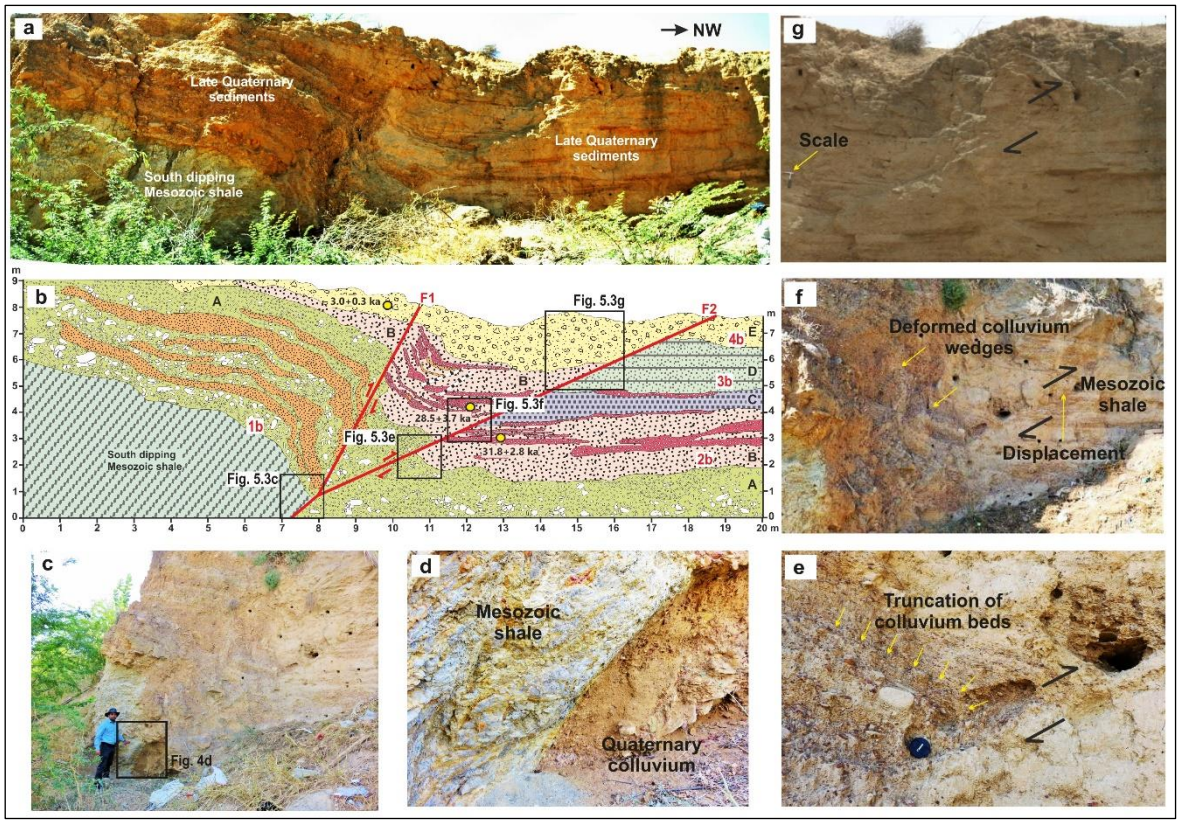

Figure 5.3 a. View of the exposure along the Khari river showing offsetting in Late Quaternary sediments overlying the KHF. Note the extension of faults up to the surface. **b.** Interpreted overlay of the section of Khari river cliff section shown in (a). (a and b modified from Patidar et al., 2008). **c.** Close view of the basal part of the section showing KHF fault plane and associated displacement of bouldery colluvium (Unit-1). **d.** Close view showing Quaternary-Mesozoic litho-contact at the base of exposed cliff section. **e.** Close view of displacement (Event-1) of older colluvial wedges along F2 fault plane. The hanging wall block clearly shows truncation of granular layers against the F2 fault plane. **f.** Enlarged view of F2 fault plane, showing displacement of mixed gravelly and sandy beds (valley-fill miliolite) of Unit-2, which corresponds to Event-2. **g.** The successively younger beds of finely laminated miliolitic sands showing displacement of Unit-3 along the fault plane, which is related to Event-3. The youngest sedimentary Unit-4, consisting of scarp derived colluvium sediments are also displaced by both the fault planes. (Modified from Patidar et al., 2008).

Based on the sediment characteristics and depositional geometry, four sedimentary units are identified from the exposed cliff section, unit 1 - Bouldery colluvium, unit 2 - Gravelly sand, unit 3 - Stratified miliolitic sand and unit 4 - Scarp-derived colluvium. The

various units described in Figure 5.3b show erosional bases labelled as 1b, 2b, 3b and 4b. However, the erosional base/ contacts 2b and 4b correspond to the major phase of erosion. They mark the major phases of erosion, which serve to categorize the total observed offset into discrete events of faulting. Based on the dip-slip displacement along the bifurcated fault planes in Quaternary sediments, three events of Late Quaternary reactivation of KHF are delineated.

Surface faulting events

Patidar et al. (2008) identified three Late Quaternary surface faulting events based on offsetting of stratigraphic units shown in Figure 5.3a, b. During each of the three faulting events, the KHF displaced the then existing topographic surface as it propagated upwards in the thin sediment cover after each Late Quaternary surface faulting event (Figure 5.4). It is obvious from the exposed cliff section that the post-faulting erosion was more severe on the southern uplifted block compared to the northern block, which has preserved larger thickness of sediments (Figure 5.4). Event 1 post-dates the deposition of Unit A during which KHF bifurcated into two faults (F1 & F2) due to rheological change as it propagated upwards from hard and compact Mesozoic rocks to unconsolidated colluvial sediments above. Erosion of the scarp formed during Event 1 precluded deposition of Units B and C. Event 2 occurred after the deposition of Unit C, which resulted in upward propagation of both F1 and F2 (Figure 5.4). The wedge-formed between these two fault planes shows evidence of severe deformation like deformed stratification and sympathetic micro-faults with offset laminations along the fault planes.

Event 2 was followed by erosion of the offset topography and deposition of stratified miliolitic sand (Unit D) and scarp derived colluvium (Unit E). Unit D is not observed in the southern uplifted block. It is believed that, either it was not deposited in the uplifted block or it was eroded off before the deposition of scarp derived colluvium (Unit E). Offsetting of Unit 6 along F1 and F2 indicates that Event 3 occurred after its deposition (Figure 5.4).

A minimum cumulative displacement of ~8 m is estimated based on the offset stratigraphy. Kundu et al. (2010) dated the section specifically with the objective of chronologically constraining the three surface faulting events delineated previously by Patidar et al. (2008). Based on optically stimulated luminescence (OSL) dating of this section carried out by Kundu et al. (2010), the three events identified are younger than 31.8 ±2.8 ka (Event 1), 28.5 ±3.7 ka (Event 2) and 3.0 ±0.3 ka BP. (Event 3).

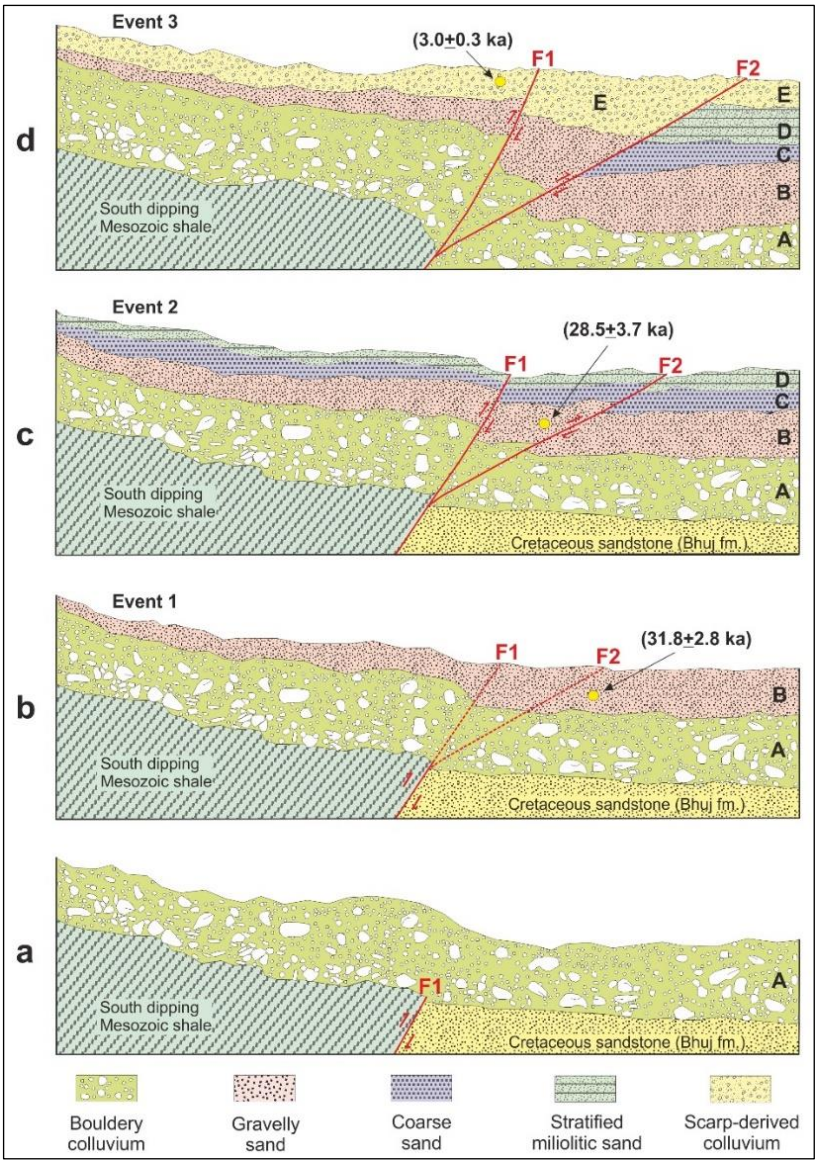

Figure 5.4 Schematic sections (not to scale) showing the occurrence of three events of Late Quaternary surface faulting along the KHF as observed in the Khari river section. Litho-units shown are the same as given in Figure 5.3a and b. All units show erosional bases suggesting post-faulting erosional intervals. Location of samples dated by Kundu et al. (2010) are also shown. **a.** Deposition of bouldery colluvium (unit A) unconformably over the Mesozoic rocks overlapping the KHF. Note the steeply southward dipping reverse movement along KHF. **b.** Deposition of gravelly sand (Unit B) over boulder colluvium and offsetting of both units (A and B) due to occurrence of surface faulting Event-1. During this event, the KHF splays into two planes (F1 and F2) as a consequence of its upward propagation in the overlying unconsolidated Late Quaternary sediments. **c.** Deposition of coarse sand (Unit C) and stratified miliolitic sand (Unit D). Comparatively higher thickness of these units is observed in the downthrown block. Deposition of this unit was followed by the occurrence of second surface faulting event (Event-2) along the KHF. **d.** Erosional interval followed by the deposition of the youngest Unit E comprising scarp-derived colluvium. This was followed by the surface faulting Event-3.

Sparse chronology of the Khari river section is, therefore, a reflection of the focused sampling by Kundu et al. (2010). As shown in Figure 5.4, the locations of dates show that Kundu et al. (2010) collected samples from the key locations only.

The three Late Quaternary surface faulting events evident in Khari river section are therefore, reasonably well constrained by the available OSL chronology (Kundu et al., 2010). The chronology of events is in agreement with the fact the sediments exposed in Khari river section reflect post-miliolite fluvial deposition (Patidar et al., 2008). $^{230}Th/^{234}U$ chronology of the aeolian miliolite deposits of the KHF zone (Baskaran et al., 1989a) indicate that aeolian miliolite deposition ceased by ~42 ka BP. This indicates that the surface faulting events seen in the stratigraphically younger fluvial sediments in Khari river section suggest occurrence of repeated surface faulting events along KHF in the past ~30 ka BP.

Displacement and Slip rate of surface faulting events

A slip history diagram according to McCalpin (2009) was constructed, which shows temporal variations in displacement at a point along the KHF in order to envisage the paleo-earthquake history of the fault (Figure 5.5).

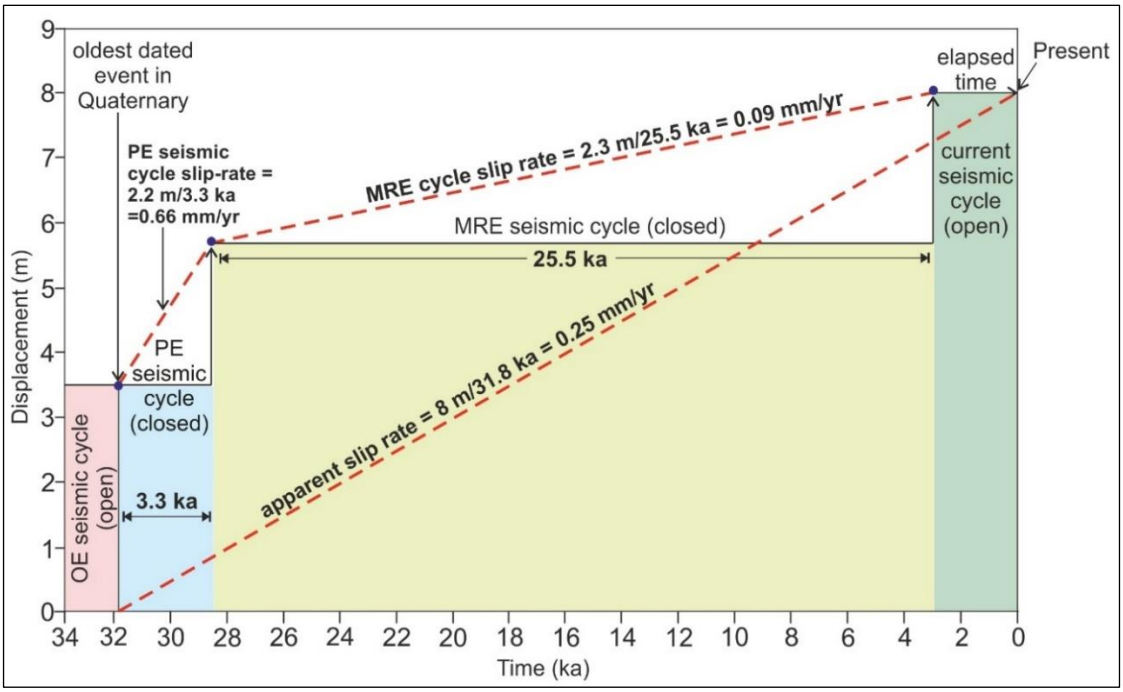

Figure 5.5 Slip history diagram of the Late Quaternary surface faulting events along KHF consisting of three paleo-earthquakes and showing two complete (closed) seismic cycles and two partial (open) seismic cycles. Diagram drawn as described by McCalpin (2009).

In this diagram, paleo-earthquake displacement plotted against time appears similar to a flight of stairs. McCalpin (2009) showed that the coseismic paleo-earthquake surface

displacement is represented by a riser between each stair and the recurrence interval is represented by the tread of each stair. The slip history diagram is not related to the smaller pre-seismic, post-seismic and inter-seismic movements of the fault (McCalpin, 2009).

The slip history diagram graphically shows the number of closed seismic cycles and parts of open seismic cycles as captured by the field paleo-seismic data (McCalpin, 2009). Figure 5.5 shows the events as mentioned in Table 5.1.

Table 5.1 Various parameters of Late Quaternary surface faulting events along the KHF as deduced in the present study.

Events	Geological Age (ka)	Rupture Length (km)	Displacement (m)	Slip-rate (mm/year)
3	3.0 ±0.3	21	2.3	0.09
2	28.5 ±3.7		2.2	0.66
1	31.8 ±2.8		3.5	--

The three paleo-earthquakes events are – the oldest earthquake (OE) at 31.8 ka with 3.5 m of displacement; the penultimate earthquake (PE) at 28.5 ka with 2.2 m of displacement while the third and most recent earthquake (MRE) occurred at 3 ka with 2.3 m of displacement. Thus, there are two complete (closed) seismic cycles, which began immediately after the OE and PE cycles and the PE cycle ended with the MRE seismic cycle. Over a period of 3.3 ka, 2.2 m of strain accumulated, which was coseismically released in the PE cycle. This yielded a closed-cycle slip rate of 2.2 m/3.3 kyr = 0.66 mm/yr. After this event, 2.3 m of strain accumulated across the fault over a period of 25.5 ka, which was then coseismically released in the MRE cycle, thus yielding a closed-cycle slip rate of 2.3 m/25.5 kyr = 0.09 mm/yr. The slip rate computed here is the actual "paleo-seismic slip rate" evaluated over two closed seismic cycles - PE and MRE cycles. McCalpin (2009) considers this slip rate to be the only "true" slip rate in the paleo-seismic history of the fault because of its property to remain constant, as the length of the two open seismic cycles in the diagram is not considered. However, if the length of the two open seismic cycles is considered in evaluating the slip rate, an "apparent slip rate" is obtained, which can get altered with the changes in the length of open seismic cycles. In the present case, the apparent slip rate determined is 0.25 mm/yr.

FIELD EVIDENCE FOR LATERAL EXTENSION OF SURFACE FAULTING

Efforts were made to trace the lateral extent of Late Quaternary surface faulting in the field by examining outcrops of Quaternary sediments lying precisely over the KHF. The objective was to determine how much length of the KHF ruptured during the Late Quaternary surface faulting visible in the Khari river section. Tectonic deformation of Late

Quaternary sediments overlying the KHF trace was taken as evidence of surface faulting. Absence of tectonic deformation in sediments meant that the KHF did not rupture in that part of the fault zone. However, the continuity of the rupture was found difficult to establish by surface mapping alone owing to the discontinuous Quaternary sediment cover attributed to the erosional topography of the arid region. The region around KHF zone can be characterised as having long recurrence interval between the seismic events (Table 5.1) as discussed in the previous chapter and experiencing erosional processes, which has resulted in the scant availability of the Quaternary sediments. In such regions, the continuity of the rupture could not be established by mere field observations, owing to the erosional topography of the area. To bridge the information gap, high-resolution geophysical technique, Ground Penetrating Radar (GPR) was used to investigate the shallow sub-surface nature of KHF and evidence of Quaternary sediment deformation. The working principle, data acquisition and processing steps required for performing and processing GPR data are discussed in Chapter – 3. Elaborate field work and GPR survey along the faulted and deformed Khari river section was performed by Patidar et al. (2008) and dating of the three surface faulting events was done by Kundu et al. (2010), which is found to be located exactly over the fault trace of KHF and is the most complete and the only stratigraphic section showing offset among the Quaternary layers. In the present chapter, few new sites displaying deformation in miliolite sediments observed in the field (marked as QD in Figure 5.2) are discussed and the interpretation of GPR data is carried out at different locations across KHF (marked as T1 to T6 in Figure 5.2) in order to locate precise trace of KHF and faulting in the shallow sub-surface comprising of Late Quaternary sediments and to appreciate the nature of faulting and deformational features related to surface faulting in the same.

South of Bharasar

An exposure of deformed Late Quaternary sediments is located to the south of Bharasar village (marked as QD in Figure 5.2), where a NE flowing lower-order tributary of Khari river shows incised Late Quaternary deposits on its eastern bank. This site is located ~3 km west to the Khari river cliff section described in the previous chapter. The older fault plane of the KHF within the Mesozoic rocks (lithotectonic contact between Bhuj and pre-Bhuj formations) is exposed across the stream bed, which is unconformably overlain by 4-5 m thick Late Quaternary sediments (colluvium followed by a stratified gravel-rich layer of valley-fill miliolite). Based on the sedimentary texture and depositional pattern, the two sedimentary units are laterally correlated with unit-2 and 3, exposed at the Khari river cliff section, located 3 km east of this section. The horizontally stratified layers of gravelly sand

unit are show truncated along a gently southward dipping fault plane in a reverse manner. Downward extension of this plane correlates with the KHF fault plane in the Mesozoic rocks exposed in the river bed (Figure 5.3a, b). Splaying nature of the KHF as seen in the Khari river section is not observed here. To understand the subsurface continuity of the fault plane and associated deformation geometries, the high-resolution GPR survey using 200 MHz frequency was carried out over the eastern bank of the stream (Figure 5.2, T4).

South of Bhujodi

An exposure of aeolian miliolite deposits, found to the south of Bhujodi village (Figure 5.6), in a shallow depression in front of the scarps effectively burying the KHF plane (marked as QD Figure 5.2).

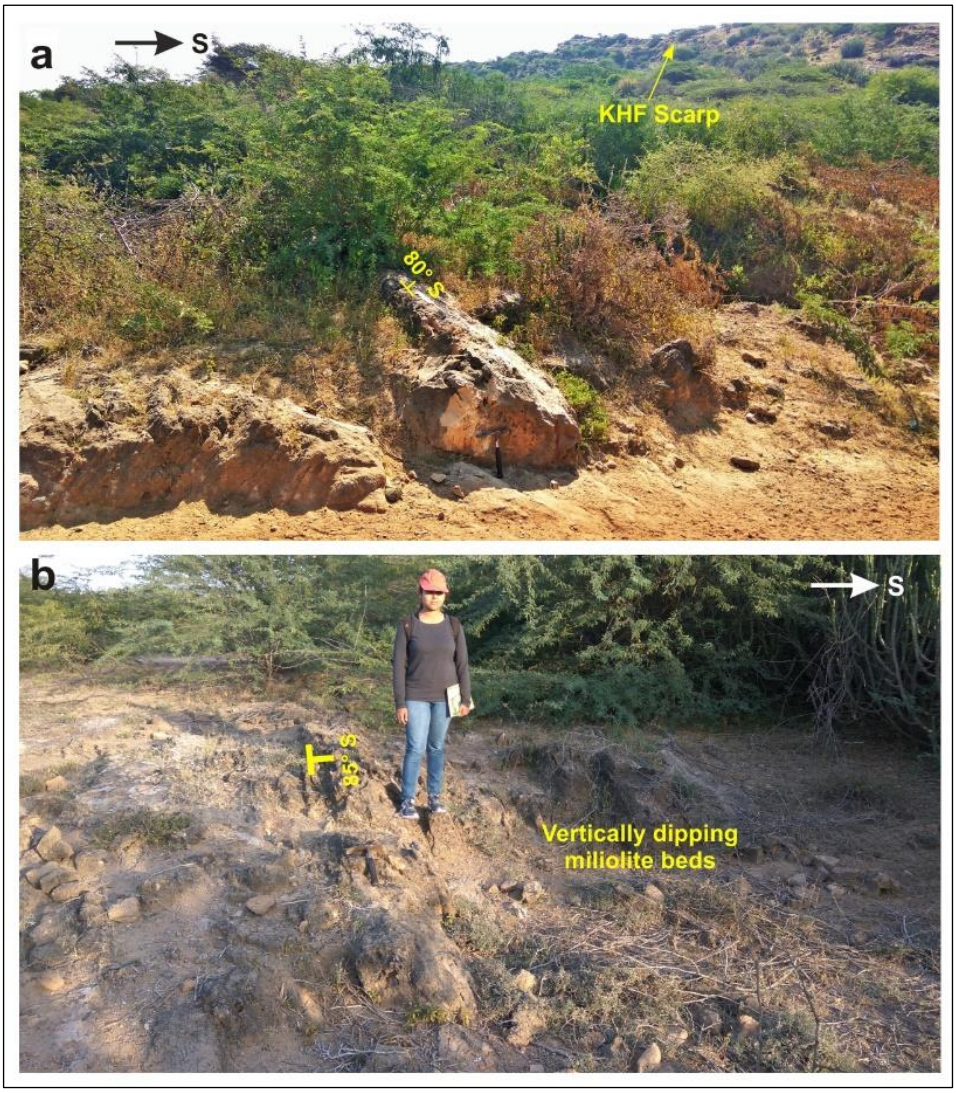

Figure 5.6 a. Tectonically deformed aeolian miliolite deposits found towards the south of Bhujodi. Note the abrupt steepening of the foresets of the cross bedding along the fault. The KHF scarp is seen in the background. Length of marker is 1.5ft. **b.** Almost vertical, south dipping stratification of aeolian miliolite deposits overlying the KHF near Bhujodi. Height of marker is 5.5ft.

The fault line of the KHF is concealed below the miliolite deposits (Figure 5.6). The aeolian characteristics of the deposit are evidenced by the large scale dunal cross-bedding of well-sorted fine grain miliolitic sand (Figure 5.6a). Above the buried fault line of KHF, an E-W trending, couple of meters wide zone showing high degree of deformation in which the dip of the foresets of thinly-laminated aeolian origin cross-bedded miliolite strata are showing near vertical dip (Figure 5.6b). This zone of deformation is laterally traceable throughout the outcrop along the buried fault trace of KHF and evident of post miliolite phase of neotectonic reactivation. Away from the KHF, the foresets attain gentle northward dips within a few tens of meters. GPR data (Figure 5.2, T3) using 200 MHz frequency is also acquired at this location to appreciate the sub-surface nature of the vertically deformed miliolite beds.

East of Shiv Paras

An outcrop displaying the contact between aeolian miliolite and Bhuj Formation is found towards the east of Shiv Paras area as shown in Figure 5.7.

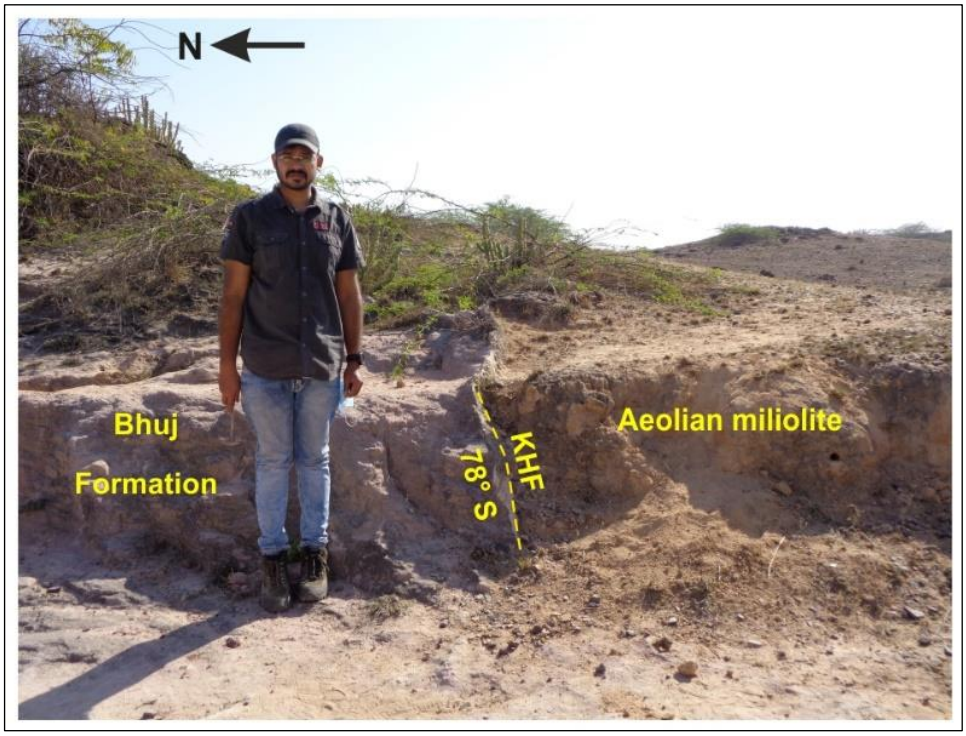

Figure 5.7 KHF plane exposed as a contact between the Bhuj Formation and aeolian miliolite deposit found east of Shiv Paras. Note the absence of macroscopic deformation in the outcrop. Height of marker is 5.6ft.

This is regarded as the exposure of the KHF plane with 78° of dip amount towards the southern direction with a roughly E-W trending strike. However, as noticed in the aeolian miliolite exposure found south of Bhujodi, this outcrop shows absence of any particular

feature related to deformation due to faulting. The exposure is rather eroded and weathered, but the contact between the two different lithologies marking the fault plane can be very well perceived.

In order to understand and confirm the subsurface continuity of fault and associated deformation geometries, the high-resolution GPR survey was carried out over the outcrops of Late Quaternary miliolite deposits found over the inferred trace of KHF to observe the effects of post-miliolite neotectonic reactivation of KHF.